film, as the field disrupts the mechanical orientation. At 94 °C there are fewer trans sequences initially, and they are increased by poling, as thermal energy and decreased interchain interactions allow dipoles to align with the applied field. Intensity changes also suggest poling may produce an improvement in packing density.

Acknowledgment. The financial support of a grant from the National Science Foundation, Polymers Program, Grant DMR No. 8407539, is deeply appreciated. We are grateful to the Pennwalt Corp. for supplying all the samples used in this study.

Registry No. (VDF)(TrFE) (copolymer), 28960-88-5.

References and Notes

(1) Lovinger, A. J. *Science (Washington, D.C.)* **1983**, *220*, 1115.
(2) Date, M.; Takashita, S.; Fukada, E. *J. Polym. Sci., Polym. Phys. Ed.* **1970**, *8*, 61.
(3) Miyata, S.; Yoshikawa, M.; Tasaka, S.; Ko, M. *Polym. J.* **1980**, *12*, 857.
(4) Maruyama, Y.; Sung Jo, Y. S.; Inoue, Y.; Chujo, R.; Tasaka, S.; Miyata, S. *Polymer* **1987**, *28*, 1087.
(5) Litt, M. H.; Hsu, C.; Basu, P. *J. Appl. Phys.* **1977**, *48*, 2208.
(6) Lovinger, A. J. *Developments in Crystalline* Polymers; Bassett, D. C., Ed.; Applied Science Publishers: Essex, U.K., 1982; p 195.
(7) Davis, G. T.; McKinney, J. E.; Broadhurst, M. G.; Roth, S. C. *J. Appl. Phys.* **1978**, *49*, 4998.
(8) Lu, F. J.; Waldman, D. A.; Hsu, S. L. *J. Polym. Sci., Polym. Phys. Ed.* **1984**, *22*, 827.
(9) Lu, F. J.; Hsu, S. L. *Polymer* **1984**, *25*, 1247.
(10) Hsu, S. L.; Lu, F. J.; Waldman, D. A.; Muthukumar, M. *Macromolecules* **1985**, *18*, 2583.
(11) Yagi, T.; Tatemoto, M.; Sako, J. *Polym. J.* **1980**, *12*, 209.
(12) Tashiro, K.; Takano, K.; Kobayashi, M.; Chatani, Y.; Tadokoro, H. *Polymer* **1981**, *22*, 1312.
(13) Lovinger, A. J.; Davis, G. T.; Furukawa, T.; Broadhurst, M. G. *Macromolecules* **1982**, *15*, 323.
(14) Davis, G. T.; Furukawa, T.; Lovinger, A. J.; Broadhurst, M. G. *Macromolecules* **1982**, *15*, 329.
(15) Lovinger, A. J.; Furukawa, T.; Davis, G. T.; Broadhurst, M. G. *Polymer* **1983**, *24*, 1233.
(16) Tashiro, K.; Takano, K.; Kobayashi, M.; Chatani, Y.; Tadokoro, H. *Polymer* **1984**, *25*, 195.
(17) Tashiro, K.; Takano, K.; Kobayashi, M.; Chatani, Y.; Tadokoro, H. *Ferroelectrics* **1984**, *57*, 297.
(18) Dvey-Aharon, H.; Sluckin, T. J.; Taylor, P. L.; Hopfinger, A. J. *Phys. Rev. B: Condens. Matter* **1980**, *21*, 3700.
(19) Furukawa, T.; Date, M.; Ohuchi, M.; Chiba, A. *J. Appl. Phys.* **1984**, *56*, 1481.
(20) Reneker, D. H.; Mazur, J. *Polymer* **1985**, *26*, 821.
(21) Tashiro, K.; Kobayashi, M. *Polymer* **1986**, *27*, 667.
(22) Guy, I. L.; Unsworth, J. *Appl. Phys. Lett.* **1988**, *52*, 532.
(23) Green, J. S.; Farmer, B. L.; Rabolt, J. F. *J. Appl. Phys.* **1986**, *60*, 2690.
(24) Stack, G. M.; Ting, R. Y. *J. Polym. Sci., Polym. Phys. Ed.* **1988**, *26*, 55.
(25) Green, J. S.; Rabe, J. P.; Rabolt, J. F. *Macromolecules* **1986**, *19*, 1725.
(26) Tashiro, K.; Kobayashi, M. *Polymer* **1988**, *29*, 426.
(27) Liang, C. Y.; Krimm, S. *J. Chem. Phys.* **1956**, *25*, 563.
(28) Moynihan, R. E. *J. Am. Chem. Soc.* **1959**, *81*, 1045.
(29) Brown, R. G. *J. Chem. Phys.* **1964**, *40*, 2900.
(30) Hannon, M. J.; Boerio, F. J.; Koenig, J. L. *J. Chem. Phys.* **1969**, *50*, 2829.
(31) Masetti, G.; Cabassi, F.; Morelli, G.; Zerbi, G. *Macromolecules* **1973**, *6*, 700.
(32) Boerio, F. J.; Koenig, J. L. *J. Polym. Sci., Polym. Phys. Ed.* **1971**, *9*, 1517.
(33) Cessac, G. L.; Curro, J. G. *J. Polym. Sci., Polym. Phys. Ed.* **1974**, *12*, 695.
(34) Kobayashi, M.; Tashiro, K.; Tadokoro, H. *Macromolecules* **1975**, *8*, 158.
(35) Tashiro, K.; Itoh, Y.; Kobayashi, M.; Tadokoro, H. *Macromolecules* **1985**, *18*, 2600.
(36) Lauchlan, L.; Rabolt, J. F. *Macromolecules* **1986**, *19*, 1049.
(37) In preparation.
(38) Davis, G. T.; Broadhurst, M. G.; Lovinger, A. J.; Furukawa, T. *Ferroelectrics* **1984**, *57*, 73.
(39) Furukawa, T.; Date, M.; Fukada, E.; Tajitsu, Y.; Chiba, A. *Jpn. J. Appl. Phys.* **1980**, *19*, L109.
(40) Yamada, T.; Ueda, T.; Kitayama, T. *J. Appl. Phys.* **1981**, *52*, 948.
(41) Lines, M. E.; Glass, A. M. *Principles and Applications of Ferroelectrics and Related Materials*; Clarendon Press: Oxford, 1977; p 103.
(42) Guy, I. L.; Unsworth, J. *J. Appl. Phys.* **1987**, *61*, 5374.

An Analysis of Phase Separation Kinetics of Model Polyurethanes

Han Sup Lee and Shaw Lind Hsu*,†

Polymer Science and Engineering Department, The University of Massachusetts, Amherst, Massachusetts 01003. *Received June 2, 1988*

ABSTRACT: Phase separation kinetics of MDI-PPO model polyurethanes have been characterized by infrared spectroscopy and DSC. The phase separation rate at temperatures between the soft segment T_g and the hard domain dissociation temperature exhibits a functional dependence that is quite similar to the well-known "bell shaped" function pertaining to crystal growth theory. The rate of phase separation was determined to be strongly dependent upon temperature. For one model polyurethane the maximum rate occurred at ~40 deg below the transition from heterogeneous to homogeneous phase. The decrease of phase separation rate at high temperatures is due to the slow initiation time. The non-Gaussian nature of the soft segment conformational distribution appears to be a contributing effect to the slow high-temperature phase separation rate. The two sets of data from infrared spectroscopy and DSC suggest a high correlation between the formation of hydrogen bonds and the overall heat flow measurable during isothermal phase separation.

Introduction

The mechanical properties of polyurethanes can be optimized by carefully choosing the types of hard[1,2] and soft segments,[1,3] molecular weight and molecular weight distribution of the two components,[4-6] synthetic method,[7,8] and the stoichiometric ratio between them.[9,10] The mechanical properties can also be dependent on the size and perfection of the phase separated morphology.[8,11] Due to the incompatibility between the hard and soft segments, polyurethane copolymers undergo microphase separation resulting in hard segment rich hard domains, soft segment rich soft matrix and an interphase between them. It is generally accepted that the strength and the elastic behavior of polyurethanes is directly related to the stability of the hydrogen-bonded hard segment rich domains, acting as junction points in the network. The existence of this heterogeneous, phase-separated structure in polyurethanes was first suggested from the mechanical behavior of the copolymer.[12] In some cases, more direct evidence have also

† To whom correspondence should be addressed.

0024-9297/89/2222-1100$01.50/0

been obtained with scattering techniques.[13-15]

Phase separation kinetics for polymer blends or block copolymers, i.e., A–B or A–B–A, have been extensively studied.[16-19] In contrast, experimental studies to characterize phase separation kinetics of segmented polyurethanes are scarce[20-22] and theoretical development for phase separation kinetics of the segmented block copolymer is also far from complete. A few techniques have been applied to study the various aspects of phase separation kinetic behavior of polyurethanes. For example, scattering technique, mainly small-angle X-ray, can give the average size of the hard domains evolving from a homogeneous single phase.[23] By monitoring mechanical properties as a function of phase separation time, the phase separation kinetics can also inferred.[24] It should be noted, however, that the direct relationship between the macroscopic mechanical properties and the degree of phase separation is generally hard to establish.

In our laboratory, vibrational spectroscopy has been used as the principal technique to characterize the different hydrogen bonds formed and to infer phase-separated structures in polyurethanes. Hydrogen bonding may form between the N—H and C=O groups of the hard segments. If polyether is part of the polymer, then hydrogen bonding between the N–H group of hard segment dispersed in the soft matrix and the C–O–C group of soft segment is also possible.[25,26] Some of the localized vibrations such as the N—H stretching vibration or C=O stretching vibration are strongly perturbed by the formation of hydrogen bonds.[27] Both the frequency shifts and intensity changes are characteristics of the specificity or magnitude of the hydrogen bonds formed. The intensity of each type of hydrogen-bonded vibration, if properly assigned, can potentially yield the degree of phase separation in the polyurethanes being studied, as reported in our earlier studies.[28,29]

Thermal analysis, mainly DSC, with some degree of success, has been applied to characterize phase separation kinetics in polyurethanes or blends.[30,31] Since the glass transition temperature of the soft segments is affected by the presence of hard segment in the soft domain, the purity of the soft domain, or the degree of phase separation, can be assessed by measuring the ΔT, defined as the temperature difference between T_g of the soft segment in the polyurethanes and T_g of the neat soft segment. More quantitative results were obtained by measuring the heat capacity change (ΔC_p) of the soft segment at glass transition temperature.[22] The ratio of the ΔC_p of the polyurethane copolymer to the ΔC_p of the pure soft segments was correlated to the degree of phase separation. Therefore, the phase separation kinetics was studied by following the changes in this ratio as a function of time.

In our study, phase separation kinetics of model segmented polyurethanes has been studied by Fourier transform infrared technique in conjunction with thermal analysis. Even though infrared technique provides information regarding the microscopic environment around each segment (functional group), it is necessary to have macroscopic information to assess the overall structural changes such as the kinetics of the domain formation. Since the thermal method that measures the heat flow during phase separation without affecting the kinetics can be used to follow the phase separation process directly, we have carried out such a study and correlated the results with the spectroscopic analysis.

Experimental Section

The model polyurethanes containing monodisperse hard and soft segments used in this study have been characterized extensively.[32] The sample used in this study contains three (B2) or five (B4) MDI units per hard segment. Butandiol was used as a chain extender. As a soft segment, poly(propylene oxide) (PPO) (VORANOL, molecular weight 2000) is used. Synthesis of the monodisperse hard segment and the resulting copolymer, shown in Figure 1, has been published previously.[32]

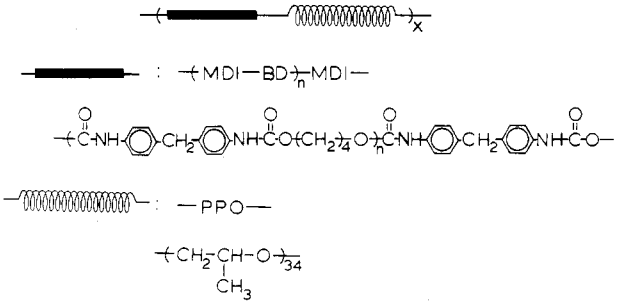

Figure 1. Schematic structure of the model polyurethanes: (top) polymer; (middle) hard segment (n = 2 and 4 correspond to B2 and B4, respectively); (bottom) soft segment.

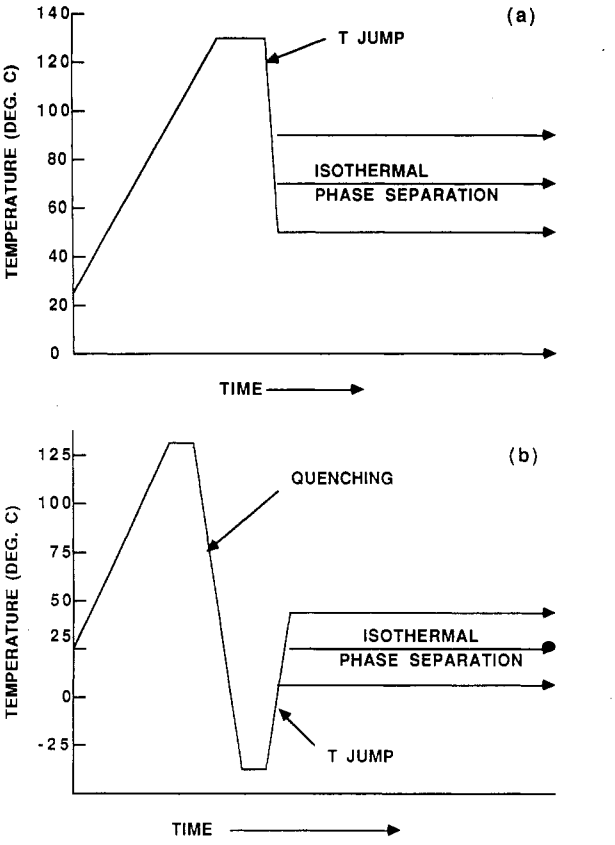

Figure 2. Temperature variations during (a) high-temperature phase separation experiments (FTIR and DSC) and (b) low-temperature phase separation experiments (FTIR).

Infrared Spectroscopic Studies. One of the key points in our experiment is our ability to obtain sampling temperature accurately and over a large range. A variable-temperature cell used in this experiment was shown earlier.[28] The temperature profiles as a function of time used in our experiment are shown in Figure 2. For high-temperature phase separation experiments as in Figure 2a, a rapid lowering of the sample temperature after initial heating can be accomplished by blowing cold N_2 gas directly onto AgCl windows. When the isothermal phase separation temperature was reached, a combination of cold and hot nitrogen gas was used to stabilize the sample temperature. For the quenching step during low-temperature phase separation experiment (Figure 2b), the liquid nitrogen is sprayed onto the windows directly while the heating cell block is cooled with the liquid nitrogen at the same time. Extremely fast quenching can be accomplished with this setup. During quenching step shown schematically in Figure 2b, samples can be cooled from 130 to −80 °C in less than 30 s. The sample temperature was measured

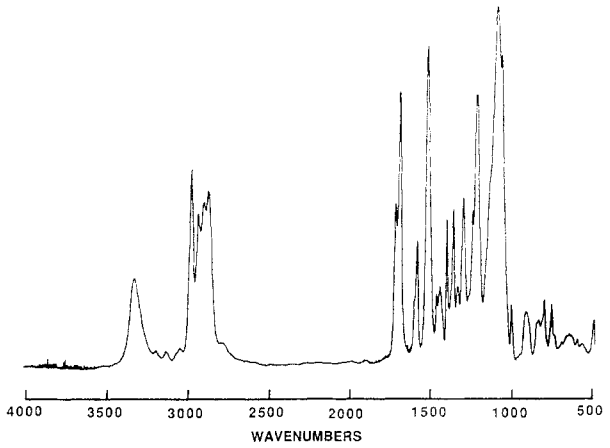

Figure 3. Infrared spectrum obtained for B2 polyurethane (2 cm^{-1} resolution; 200 scan; room temperature).

directly with a copper–constantan thermocouple held between the two windows. Films suitable for spectroscopic studies were obtained by casting 2% (w/v) solution in THF directly on the AgCl salt plate. It was slowly dried for 24 h in atmosphere until most of the solvent evaporated and then vacuum dried at 70 °C for a few days.

All the infrared spectra were obtained with an IBM Model 98 vacuum Fourier transform infrared spectrometer. Spectral resolution is maintained at 2 cm^{-1}. In two experiments, at 45 and 55 °C, when high time resolution was required to follow the high rate of phase separation, we reduced the spectral resolution to 4 cm^{-1}. Although there are multiple bands of interest in the carbonyl stretching region, we have not carried out band deconvolution because of uncertain band width, differences in the inherent extinction coefficients, and the number of components present.[33] Since the peak position of the carbonyl band at approximately 1730 cm^{-1} shows little shift during isothermal phase separation, it is assumed that band height measurements can be used to represent the changing band intensity as a function of time without significant error. When more reliable band assignments become available, deconvolution procedures can be applied. Infrared spectrum of the B2 model polyurethane at room temperature is shown in Figure 3.

Thermal Analysis. Since it was difficult to change the temperature quickly without significant overshooting, only high-temperature phase separation kinetic studies were reliably carried out with DSC. The same samples as used in infrared measurements were studied. A Perkin-Elmer DSC-7 calorimeter controlled by a Perkin-Elmer 7500 computer was used with indium standard. Phase mixing was initially obtained by heating the sample to ~130 °C, which is above the hard-domain dissociation temperature (T_d). Since the phase separation rate above 100 °C was very slow, the temperature was lowered from 130 to 100 °C slowly and equilibrated for 10 min, before being quenched to isothermal phase separation temperature, in order to minimize the transient state during temperature change. After lowering to the isothermal phase separation temperature, heat flow was monitored isothermally as a function of time.

Results and Discussion

Spectroscopic Study of Phase Separation Kinetics. The stable hard segment rich domains in polyurethanes are characterized by interurethane C=O···H—N hydrogen bonds. The typical room-temperature infrared spectrum obtained for our samples in the carbonyl stretching region shows two distinct peaks (Figure 4). The time equals zero spectrum is the start of the first spectrum we collect after the quenching. The peak at 1730 cm^{-1} is assigned to the free carbonyl peak, and the clearly distinguishable one at 1700 cm^{-1} is assigned to carbonyl groups hydrogen bonded to N–H group. The generally higher absorbance observed for the 1700 cm^{-1} peak relative to the 1730 cm^{-1} component is characteristic of a typical phase-separated structure of polyurethanes.

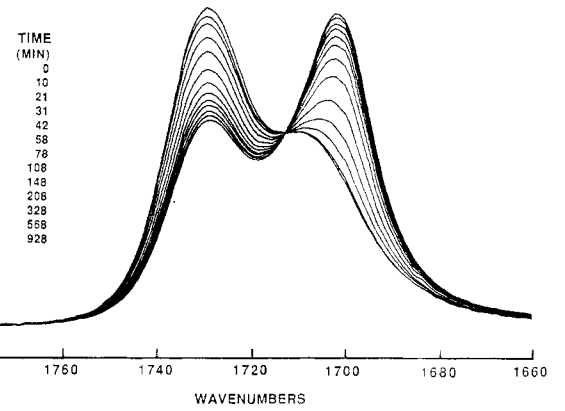

Figure 4. Changes observed as a function of isothermal phase separation time for the C=O stretching region of B2 polyurethane at 15 °C. Spectrum obtained at $t = 0$ has low absorbance at 1700 cm^{-1} and high absorbance at 1730 cm^{-1}.

If the model B2 polyurethane is heated above the hard domain dissociation temperature (~100 °C),[32] the relative intensity of the two carbonyl peaks changes significantly as the heterogeneous structure transforms to a homogeneous one. Since most of the hard segments in the homogeneous state are surrounded by the soft segments, the carbonyl groups are free of hydrogen bonding as characterized by the high absorbance of the 1730 cm^{-1} peak. As we have demonstrated previously, this phase mixed state can be preserved at extremely low temperatures by rapidly quenching the sample to below the glass transition temperature of the soft segments.[28,29]

Isothermal phase separation kinetics can then be studied by raising the sample temperature quickly to the phase separation temperature and measure the changes in the infrared spectrum at constant temperature. When a homogeneous structure phase separates, the carbonyl group is transformed from a free state to a state hydrogen bonded to a N–H group. Changes in the carbonyl region during isothermal phase separation are shown in Figure 4 as a function of time. Since the 1730 cm^{-1} peak is assigned to the free carbonyl peak, high absorbance value of that component indicates a high degree of phase mixing at time zero. As isothermal phase separation proceeds, the 1700 cm^{-1} component, assigned to carbonyl groups hydrogen bonded to N–H, increases, while the 1730 cm^{-1} component decreases in intensity. Our data clearly indicate that the phase separation process involves a gradual transfer of the hard segments dissolved in the soft matrix into the hard domain. It should be noted that our data are obtained at a constant temperature. Previous studies have shown that frequency and intensity differences at different temperatures for both the hydrogen bonded and free C=O vibrations can be significant and difficult to define.[34,35] Measuring the relative intensity of the two components at constant temperature removes this difficulty.

In our analysis, the peak intensity of the 1730 cm^{-1} component is used to obtain fractional degree of phase separation as shown in Figure 5. Typically, after a short slow initiation period, phase separation increases rapidly above an approximately 70% degree of phase separation and then decreases before reaching the maximum degree of phase separation asymptotically. The data plotted in Figure 5 resemble a crystallization isotherm, even though they deviate slightly from the usual sigmoidal shape for data obtained at later stages of phase separation. It is also apparent that fractional phase separation is very sensitive to the temperature.

In theory, the N—H stretching vibration should also yield complementary structural information to the C=O

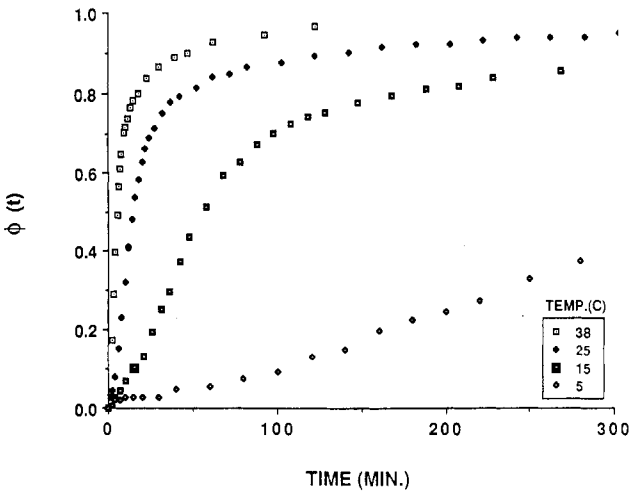

Figure 5. Decrease in the 1730 cm^{-1} (increase of 1700 cm^{-1}) component as a function of time at four different temperatures. $\phi(t)$ denotes the fractional degree of phase separation and is calculated as $(I(t) - I(0)/I(\infty) - I(0))$ where $I(0)$, $I(t)$, and $I(\infty)$ being intensity of 1730 cm^{-1} component at phase separation time zero (just after quenching), t, and infinity (extrapolated), respectively.

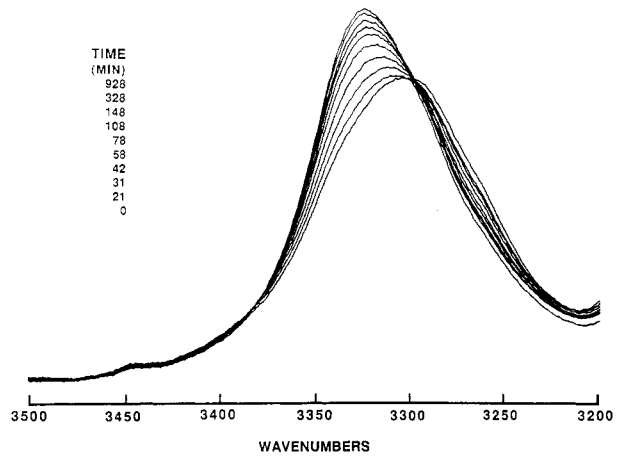

Figure 6. Changes observed as function of isothermal phase separation time for the N-H stretching region of B2 polyurethane at 15 °C. Spectrum obtained at $t = 0$ has low absorbance at 3330 cm^{-1}.

stretching vibration. N—H groups can form hydrogen bonding with C=O group of the hard segments as well as ether group of the soft segment. This vibration, however, is complicated by not only the two types of hydrogen bonding observed but also other second-order spectroscopic effects involving the N-H stretching fundamental and combinations of lower lying amide vibrations.[36] Changes in N-H stretching region during corresponding isothermal phase separation process is shown in Figure 6. Even though spectral complications do not allow a simple quantitative analysis, changes occurring during isothermal phase separation as shown in Figure 6 can be understood qualitatively because the temperature effect is removed.

Generally speaking, the frequency of N-H groups free from hydrogen bonding is at 3450 cm^{-1}. The extremely weak 3450 cm^{-1} peak in Figure 6 indicates that most of the N-H group is hydrogen bonded with either hard segment or soft segment. We have assigned 3330 and 3295 cm^{-1} bands to N—H groups hydrogen bonded to C=O groups and the ether oxygens, respectively.[28] The number of N—H···C—O—C(ether) hydrogen bonds should diminish, with a corresponding increase in the number of N—H··· C=O bonds during isothermal phase separation. We expect, then, the 3330 cm^{-1} component is to increase and the

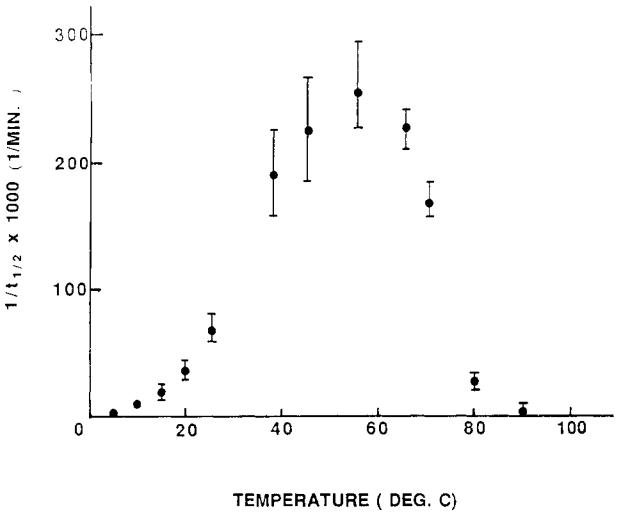

Figure 7. Phase separation rate of B2 polyurethane as a function of temperature. $t_{1/2}$ is the time for 50% phase separation (refer, for example, to Figure 5).

3295 cm^{-1} component to decrease in intensity as a function of time. In most cases these two components are difficult to separate cleanly. The decrease of the 3295 cm^{-1} component is only seen as a decreasing shoulder due to the broad nature of the peak (refer to time zero spectrum of Figure 6). The increase of the 3330 cm^{-1} peak, however, is quite obvious. As phase separation proceeds, it grows from a weak shoulder into the dominant peak clearly indicating the formation of the hydrogen bonding between the hard segments, i.e., hydrogen bonding between N—H group and C=O group.

The phase separation rate can be obtained generally from the time required to achieve a 50% phase separation, $t_{1/2}$. The rates for each temperature can be obtained from the data presented in Figure 5 and are summarized in Figure 7. The temperature range we have selected for our rate measurement was from 0 to 100 °C. The selection of the this range was determined by the glass transition temperature of the soft segments and the dissociation temperature of the hard domain. The phase separation rate data over this temperature range of the segmented polyurethane has not been reported previously. Our plotted data shown in Figure 7 resemble the behavior of the crystallization rate as a function of temperature.

Crystal growth can be represented by eq 1

$$G = G_0 \exp\left(\frac{-A}{R(T - T_0)}\right) \exp\left(-\frac{BT_m}{T\Delta T}\right) \qquad (1)$$

where G_0 is a constant, A the activation energy associated with segmental motions, T_0 a temperature below the glass transition temperature, $\Delta T = (T_m - T)$ the undercooling, and B a constant defined as $4b_0\sigma\sigma_e/\Delta H_f$ in the case corresponding to a two-dimensional crystal growth.[37] σ and σ_e refer respectively to the lateral and fold surface free energies of the polymer crystal and ΔH_f molar enthalpy of fusion. The first exponential function relates to the chain mobility and takes into account the movement of matter from the melt to the crystal surface. The second exponential function originates from the nucleation process.

We feel there is a close analogy between the formation of hard domain from the "homogeneous" mixed phase during phase separation and the formation of a crystalline phase from the homogeneous melt during crystallization. Therefore, Figure 7 can be understood qualitatively in terms of eq 1 which explains the slow rates at low and high

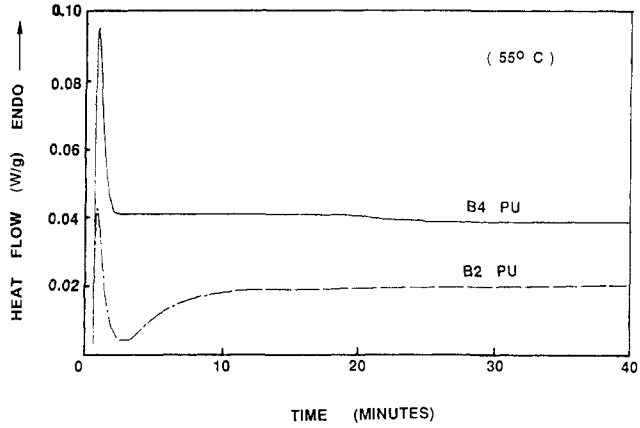

Figure 8. DSC traces for two (B2 and B4) polyurethanes during isothermal (55 °C) phase separation. $t = 0$ corresponds to time just after quenching to phase separation temperature. Transient state after quenching is observed for both samples.

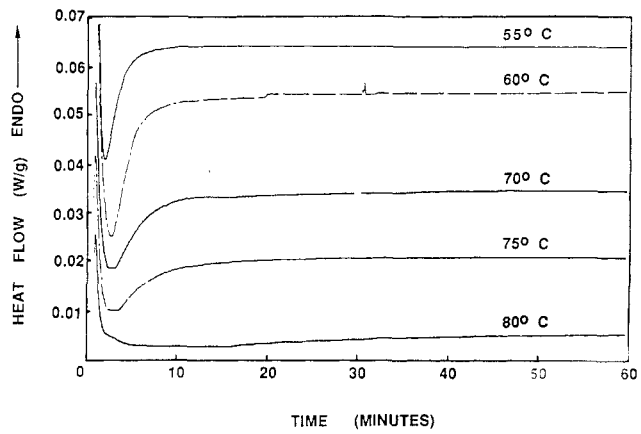

Figure 9. DSC traces of B2 polyurethanes during isothermal phase separation.

temperatures and relatively faster rates at intermediate temperatures.

It should be noted that the fully phase separated B2 polyurethane does not show any birefringence through a cross-polarizing optical microscope. Furthermore, wide-angle X-ray diffraction patterns of B2 model polyurethanes also do not show any crystalline peak, even when the sample is well annealed above the glass transition temperature of the soft segment.[32] Therefore, the spectral changes with time in Figure 4 are due to phase separation process not to crystallization.

The slowing of the phase separation rate at high temperatures then needs to be explained further. One possibility is the fact that hard segment movements may meet resistance from the contractile force of the soft segments. The stress, σ, for N_c network chains as a function of strain, α, in the case of uniaxial stretching at constant volume, can be expressed as eq 2.

$$\sigma = kT(N_c/V)(\alpha^2 - 1/\alpha) \qquad (2)$$

The contractile force at constant extension ratio is proportional to the temperature. Since the flexible soft segment is shown to exist in an extended state for the phase-separated structure,[38-40] the force against phase separation at high temperature will be expected to be higher, thus slowing phase separation. The slow phase separation rate at the high-temperature side of Figure 7 is, therefore, thought to be affected by the loss of conformational entropy of the soft segment when phase separated.

Thermal Analysis of Phase Separation Kinetics. DSC traces during isothermal phase separation for two different samples are shwon in Figure 8. A clear endothermic peak during heating process was observed for the annealed B2 model polyurethane. The presence of an exothermic peak during the isothermal phase separation of the B2 sample was observed, indicating that heat flow during isothermal phase separation can be detected with the DSC technique. The B4 model polyurethane is partially crystalline and undergoes a transition from heterogeneous to homogeneous phase around 170 °C.[32] Since both samples were heated only to 130 °C, the exothermic peak was not observed for the B4 sample. Accordingly the difference in DSC traces between B2 and B4 is purely due to the phase separation process of the B2 sample (refer to Figure 8). The dissociation energy of the hydrogen bond is known to be in the range of 5–8 kcal/mol.[41] Since the C=O···H—N hydrogen bonds are formed during isothermal phase separation, it is not surprising that the exothermic peak has been detected. As we have suggested earlier, the interurethane hydrogen bonds are replacing some of the N-H···O- hydrogen bonds.[28,29] The disruption of the latter must be considered as well. The frequency of the N—H···—O- band seems to suggest that this hydrogen bond is in fact stronger than C=O···H—N at room temperature or below. It has also been noted that the hydrogen bonding between hard segment and soft segment becomes less stable at the high temperatures used during DSC experiments.[28] Since the C=O···H—N bond is formed at the expense of the less stable N—H···—O- (ether) bond during phase separation at high temperature, an exothermic peak, not an endothermic, is then expected. The free energy difference before and after phase separation and nonbonded interactions due to other secondary forces are believed to contribute to the overall heat flow during isothermal phase separation even though they are not considered to be major factors.

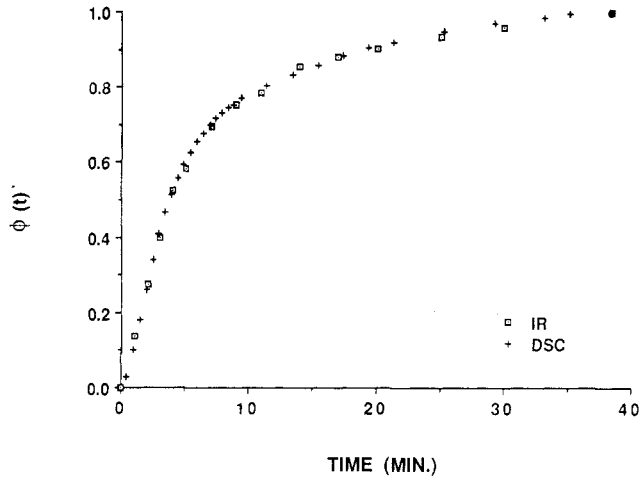

Figure 10. $\phi(t)$ as a function of isothermal (70 °C) phase separation time. $\phi(t)$ is obtained as $(I(t) - I(0))/(I(40) - I(0))$ where $I(t)$ is the absorbance of 1730 cm^{-1} component for the FTIR data and exothermic energy evolved up to time t for the DSC data.

Exothermic peaks during isothermal phase separation at several different temperatures are shown in Figure 9. Spectroscopic data shown in Figure 7 indicate that the phase separation rate is at a maximum around 55 °C and then decreases as temperature increases. Figure 9 shows exactly the same tendency. The exothermic peak becomes wider and shallower as the temperature increases from 55 to 80 °C, indicating that phase separation rate progressively becomes slower as temperature increases above 55 °C.

Fractional degrees of phase separation obtained at 70 °C with two different techniques, i.e., infrared and DSC, are shown in Figure 10. Even though infrared and DSC technique measure very different structural features, Figure 10 indicates that there is a strong correlation between segmental interaction, mainly hydrogen bonding, and macroscopic thermal characteristics. Since infrared technique detects the formation of hydrogen bonding between hard segments and DSC technique measures the energy generated by the formation of hydrogen bonding, it is not unexpected to have consistent results between the two techniques.

Conclusions

The phase separation kinetics data shown in Figure 7, we believe, is one of the first complete set of experimental work for segmented polyurethanes. The infrared phase separation kinetics data are supported with DSC data. Even though the wide-angle X-ray scattering (WAXS) pattern shows no crystallinity in B2 polyurethane, the exothermic peak observed during isothermal phase separation indicates that the formation of new segmental interactions, mainly hydrogen bonding, can be detected. Care must be exercised in carrying out the phase separation kinetic experiment since the exothermic peak is very small. In case of phase separation without formation of strong secondary bonds, the signal is expected to be even smaller making the thermal analysis for direct information extremely difficult.

The phase separation mechanism has been discussed previously.[29] Our spectroscopic data do not seem to satisfy the linearized Cahn–Hilliard spinodal decomposition equation. It is well-known that spontaneous phase separation may not be possible, even for the unstable region, if high interfacial energy is required.[42] In the case of segmented polyurethanes, high coherent interfacial energy is required due to the connectivity of the chains which run through the multiple soft and hard domains. The lack of spinodal mechanism over a wide range of temperature in this case, therefore, may be due to the high interfacial energy. To reach a concrete conclusion, we need additional experimental data as well as theoretical development which shows the effect of high interfacial energy on the spinodal decomposition mechanism for segmented block copolymers.

Acknowledgment. We are extremely grateful to the financial support from the National Science Foundation, Polymers Programs, DMR-8407539, and one from US—China Cooperative Grant INT-8713724. H.S.L. is appreciative of a fellowship from the Dow Chemical Corp. We particularly want to thank Drs. C. Christenson, W. M. Lee, and M. Harthcock for helpful discussions and Dr. D. S. Lee for the assistance during DSC experiment.

Registry No. (MDI)(PPO)(Bl) (blocker copolymer), 106208-51-9.

References and Notes

(1) Pigott, K. A.; Frye, B. F.; Allen, K. R.; Steingiser, S.; Darr, W. C.; Saunders, J. H.; Hardy, E. E. *J. Chem. Eng. Data* **1960**, *5*, 391.
(2) MacKnight, W. J.; Yang, M. *J. Polym. Sci., Polym. Symp.* **1973**, *42*, 817.
(3) Bayer, O.; Mueller, E.; Petersen, S.; Piepenbrink, H. F.; Windemuth, E. *Rubber Chem. Technol.* **1950**, *23*, 812; *Angew. Chem.* **1950**, *62*, 57.
(4) Harrell, L. L. *Macromolecules* **1969**, *2*, 607.
(5) Ng, H. N.; Allegrezza, A. E.; Seymour, R. W.; Cooper, S. L. *Polymer* **1973**, *14*, 255.
(6) Miller, J. A.; Lin, S. B.; Hwang, K. K. S.; Wu, K. S.; Gibson, P. E.; Cooper, S. L. *Macromolecules* **1985**, *18*, 32.
(7) Abouzahr, S.; Wilkes, G. L. *J. Appl. Polym. Sci.* **1984**, *29*, 2695.
(8) Camargo, R. E.; Macosko, C. W.; Tirrell, M.; Wellinghoff, S. T. *Polymer* **1985**, *26*, 1145.
(9) Schneider, N. S.; Sung, C. S. P.; Matton, R. W.; Illinger, J. L. *Macromolecules* **1975**, *8*, 62.
(10) Abouzahr, S.; Wilkes, G. L.; Ophir, Z. *Polymer* **1982**, *23*, 1077.
(11) Serrano, M.; Macknight, W. J.; Thomas, E. L.; Ottino, J. M. *Polymer* **1987**, *28*, 1667.
(12) Cooper, S. L.; Tobolsky, A. V. *J. Appl. Polym. Sci.* **1966**, *10*, 1837.
(13) Shimanskii, V. M.; Shkol'nik, S. I.; Kozakov, S. B. *Sov. Rubber Technol. (Engl. Transl.)* **1967**, *26*, 20.
(14) Clough, S. B.; Schneider, N. S.; King, A. O. *J. Macromol. Sci., Phys.* **1968**, *B2*, 641.
(15) Bonart, R.; Morbitzer, L.; Hentze, G. *J. Macromol. Sci., Phys.* **1969**, *B3*, 337.
(16) Gaur, U.; Wunderlich, B. *Macromolecules* **1980**, *13*, 1618.
(17) Yang, H.; Shibayama, M.; Stein, R. S.; Shimizu, N.; Hashimoto, T. *Macromolecules* **1986**, *19*, 1667.
(18) Leibler, L. *Macromolecules* **1980**, *13*, 1602.
(19) Mori, K.; Tanaka, H.; Hashimoto, T. *Macromolecules* **1987**, *20*, 381.
(20) Wilkes, G. L.; Bagrodia, S.; Humphries, W.; Wildnauer, R. *J. Polym. Sci., Polym. Lett. Ed.* **1975**, *13*, 321.
(21) Hesketh, T. R.; Van Bogart, J. W. C.; Cooper, S. L. *Polym. Eng. Sci.* **1980**, *20*, 190.
(22) Camberlin, Y.; Pascault, J. P. *J. Polym. Sci., Polym. Phys. Ed.* **1984**, *22*, 1835.
(23) Wilkes, G. L.; Emerson, J. A. *J. Appl. Phys.* **1976**, *47*, 4261.
(24) Wilkes, G. L.; Wildnauer, R. *J. Appl. Phys.* **1975**, *46*, 4148.
(25) Boyarchuk, Y. M.; Rappoport, L. Y.; Nikitin, V. N.; Apukhtina, N. P. *Polym. Sci. USSR (Engl. Transl.)* **1965**, *7*, 859.
(26) Yokoyama, T. *Adv. Urethane Sci. Technol.* **1975**, *6*, 1; Frisch, K. C., Reegen, S. L., Eds.
(27) Coleman, M. M.; Lee, K. H.; Skrovanek, D. J.; Painter, P. C. *Macromolecules* **1986**, *19*, 2149 and references therein.
(28) Lee, H. S.; Wang, Y. K.; Hsu, S. L. *Macromolecules* **1987**, *20*, 2089.
(29) Lee, H. S.; Wang, Y. K.; MacKnight, W. J.; Hsu, S. L. *Macromolecules* **1988**, *21*, 270.
(30) Chee, K. K.; Farris, R. J. *J. Appl. Polym. Sci.* **1984**, *29*, 2529.
(31) Kwei, T. K. *J. Appl. Polym. Sci.* **1982**, *27*, 2891.
(32) Christenson, C. P.; Harthcock, M. A.; Meadow, M. D.; Spell, H. L.; Howard, W. L.; Creswick, M. W.; Guerra, R. E.; Turner, R. B. *J. Polym. Sci., Polym. Phys. Ed.* **1986**, *24*, 1401.
(33) Skrovanek, D. J.; Howe, S. E.; Painter, P. C.; Coleman, M. M. *Macromolecules* **1985**, *18*, 1676.
(34) Koberstein, J. T.; Gancarz, I. *J. Polym. Sci., Polym. Phys. Ed.* **1986**, *24*, 2487.
(35) Skrovanek, D. J.; Painter, P. C.; Coleman, M. M. *Macromolecules* **1986**, *19*, 699.
(36) Suzuki, S.; Iwashita, Y.; Shimanouchi, T.; Tsuboi, T. *Biopolymers* **1966**, *4*, 337.
(37) Hoffman, J. D.; Weeks, J. J. *J. Chem. Phys.* **1962**, *37*, 1723.
(38) Hashimoto, T.; Shibayama, M.; Kawai, H. *Macromolecules* **1983**, *16*, 1093.
(39) Miller, J. A.; Pruckmayr, G.; Epperson, E.; Cooper, S. L. *Polymer* **1985**, *26*, 1915.
(40) Miller, J. A.; Cooper, S. L.; Han, C. C.; Pruckmayr, G. *Macromolecules* **1984**, *17*, 1063.
(41) Pimentel, G. C.; McClellan, A. L. *The Hydrogen Bond*, W. H. Freeman: San Francisco, 1960.
(42) Hilliard, J. E. *Phase Transformations*, Cohen, M., Ed.; ASM, 1968; Chapter 12.